

## The NAC Proton Therapy Beam Delivery System

A.N. SCHREUDER, D.T.L. JONES, J.E. SYMONS, T. FULCHER and A. KIEFER.

National Accelerator Centre, PO Box 72, Faure, 7131 SOUTH AFRICA

The 200 MeV horizontal proton therapy beam line at the NAC was commissioned in September 1993 and a total of 98 patients had been treated up to September 1995. The present proton beam delivery system is designed for a maximum field diameter of 100 mm and was optimized for plateau crossfire irradiations. The beam exits the vacuum system 7 m from the isocentre. A double scatterer plus occluding ring system is used to flatten the beam while a rotating variable-thickness absorber spreads out the Bragg Peak. The position of the beam is controlled by two computerized feedback systems acting on two sets of XY steering magnets. Positional information is obtained from quadrant and multiwire ionization chambers. The dose to the patient is monitored by two parallel plate ionization chambers immediately upstream of the final patient collimator. A real time range monitor gives a continuous indication of the range of the incident protons and hence the beam energy.

### 1. Introduction

The 200 MeV horizontal beam proton therapy facility at the NAC was initially designed for plateau (shoot-through) irradiations of intracranial lesions.<sup>1</sup> The first patient was treated on 10 September 1993 using this technique. The necessary facilities for full spread-out Bragg peak (SOBP) treatments were installed early in 1994, and since then this became the treatment of choice for the majority of the proton treatments at the NAC facility, except for small ( $\leq 20$  mm diameter) lesions.

### 2. The proton beam line layout

A schematic layout of the beam delivery system is shown in figure 1. Due to the design and movements of the treatment chair, it was necessary to mount the front end components of the beam line from a cantilever system as shown in figure

1. These components are mounted on linear bearings and can be moved upstream along the beam line as well as sideways out of the beam to make room for the treatment chair and to allow for the coaxial laser to indicate the beam position. Most of the other beam line components are also mounted on bearings on an accurate optical bench and their positions can easily be changed for experimental purposes. For treatment purposes, the position of each device is interlocked to ensure that the correct components are in the beam.

The total distance between the vacuum window and the isocentre is 7 meters. The proton beam exits the vacuum through a 0.025 mm thick Havar window. A double scatterer plus occluding ring system<sup>2</sup> is used to flatten the proton beam and was designed using the NEU program made available to the NAC by Gottschalk.<sup>3</sup>

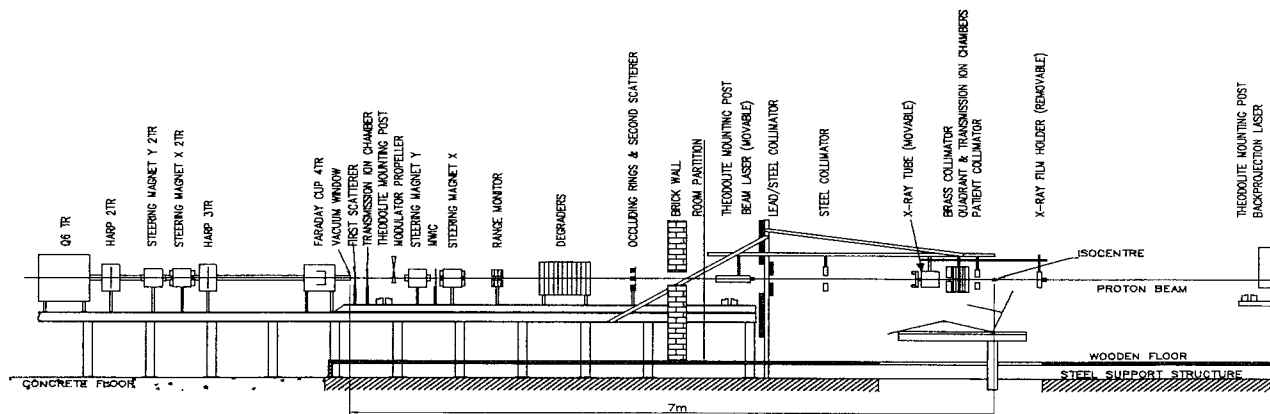


Figure 1: A schematic layout of the proton beam delivery system.

The beam delivery system is designed for a maximum field diameter of 100 mm. The first scatterer is located immediately downstream of the vacuum window and is a 1 mm thick lead plate. The occluding rings (50 mm thick brass) are mounted on the second scatterer which is a 1 mm thick brass plate and are 2.9 m downstream of the first scatterer. The central stopper has a radius of 1.344 cm while the inner and outer radii of the concentric ring are 2.418 and 3.611 cm respectively. This beam-spreading system is currently used for all field sizes. The design criteria stipulated a flat beam i.e. less than  $\pm 2.5\%$  variation in dose over 80 % of the beam area which is defined at the FWHM, for a 100 mm diameter beam at the isocentre. It was furthermore important to preserve the beam energy as much as possible to allow plateau irradiations i.e. to maximize the range of the protons.

The double scattering system being used is extremely sensitive to the beam position and it was found essential to install an automated control system. The beam is controlled by two computerized feedback systems acting on two sets of XY steering magnets. The first feedback system uses a multiwire ionization chamber (MWIC) with 2 mm resolution which monitors the beam position in the X and Y planes perpendicular to the beam direction. The MWIC is located 85 cm downstream of the vacuum window. Positional information from this chamber is fed back to a set of XY steering magnets 280 cm upstream of the MWIC.

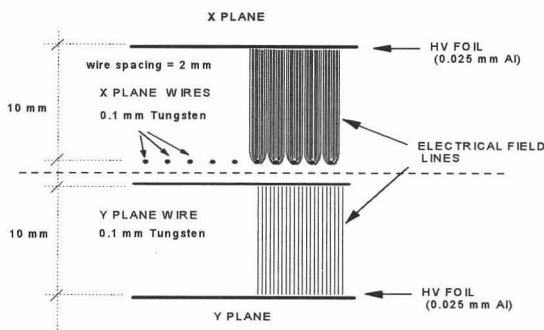


Figure 2: A schematic layout of the MWIC.

The MWIC consists of a set of 49 tungsten wires in both the X and Y planes respectively. The wires are spaced at 2 mm intervals and are 0.1 mm in diameter. Each set of wires has its own high voltage plate at a distance of 10 mm from the wire plane. A polarizing voltage of +500 V is applied to each high voltage plate while each of the wires is connected to virtual earth through a measuring device. Ionizations in the vicinity of a wire will be recorded as a current on that wire. The MWIC is mounted very accurately in the beam line in such a way that the central wires in both planes align with the beam axis. A schematic layout of the MWIC is shown in figure 2.

The second feedback system uses the signals from a segmented (quadrant) transmission ion chamber (Lawrence Berkeley Laboratory) which monitors the beam symmetry and is located close to the patient. The positional information from the quadrant chamber is used to adjust another set of XY steering magnets which are located on each side of the MWIC. The first feedback system therefore ensures that the beam is aligned with the beam axis at the position of the MWIC which can be seen as a beam pivot point. The dual feedback system ensures a very stable and symmetrical beam. Symmetries of  $\leq 1\%$  are routinely obtained.

There are 4 anti-scatter collimators in the beam as shown in Fig. 1. The final (patient) collimator is located 27.5 cm upstream of the isocentre. Fixed inserts, which can either be custom-made or of a standard shape, fit into the final collimator assembly which can rotate around the beam axis in order to align non-circular collimators with the required treatment field. These inserts are made of brass (5 cm thick) or low-melting-point alloy (6 cm thick). A co-axial x-ray tube is mounted upstream of the patient collimator assembly and is used for portal x-ray radiographs. These radiographs are compared with Digitally Reconstructed Radiographs (DRRs) obtained from the treatment planning system to verify the final set-up position of the patient and the collimator rotation angle. Front- and back-pointer lasers are used to indicate the beam axis while the field light from the co-axial x-ray unit is sometimes used to project the shape of the final collimator onto the patient. Lateral lasers are also provided.

There are mounting posts at various positions along the beam axis for locating a theodolite, which is used for precise alignment of the beam line components and for accurately checking the patient position if required. A dual transmission ionization chamber system (5  $\mu\text{m}$  thick aluminized mylar foils, 5 mm separation) located immediately upstream of the patient collimator is used to monitor the dose delivered. A single transmission ionization chamber (5  $\mu\text{m}$  thick aluminized mylar foils, 1 mm separation) located immediately downstream of the first scatterer is used for experimental purposes. All these monitors are filled with ambient air.

The transmission ionization chambers used for dose monitoring are calibrated against air-filled A150 tissue-equivalent ionization chambers according to the "Code of practice for clinical proton dosimetry".<sup>4,5</sup> Dose rates which have been used clinically for plateau irradiations are about 3 Gy.min<sup>-1</sup> (measured at a depth of 5 cm in water) corresponding to a cyclotron beam current of about 15 nA. For a typical SOBP beam with a range of 120 mm in water,  $\pm 35$  nA of incident proton beam current is required to obtain the same dose rate in the center of the SOBP region. The total mass in the path of the beam between the vacuum system and the isocentre is about 2.0 g.cm<sup>-1</sup> corresponding

to an energy loss of about 9 MeV for a beam with a nominal incident energy of 200 MeV. Since the beam energy cannot be reproduced exactly week by week plastic range shifter plates,  $0.6 \text{ g.cm}^{-2}$  thick, are placed upstream of the range monitor in order to routinely produce a residual range of  $24.00 \pm 0.03 \text{ cm}$  in water (distal 50% level) for patient treatment. For SOBP therapy additional acrylic degrader plates are inserted just downstream of the range monitor to obtain the required range.

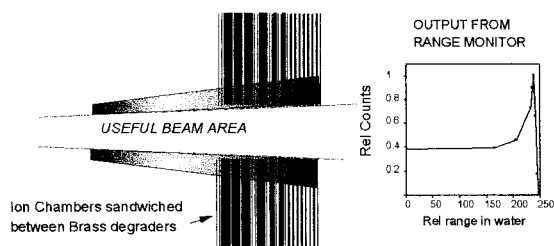


Figure 3: A schematic layout of the real time range monitor.

A range monitor was designed and constructed to measure the proton range in brass and hence the incident proton energy in real time. A schematic layout of this monitor is shown in figure 3. The monitor consists out of 12 transmission parallel plate ionization chambers, made from PC board material. These chambers are sandwiched between brass plates. Each ionization chamber and brass plate has a 100 mm hole in the center. The total thickness of the ionization chamber plates and brass plates is more than the maximum range of the incident protons in these materials. The full width at half maximum (FWHM) of the proton beam at the position of the range monitor is greater than the 100 mm inner diameter of the range monitor. This means that the range monitor also acts as an anti-scatter collimator. The useful beam passes unaltered through the range monitor while the redundant protons are stopped in the brass plates and ionization chamber materials. The ionization currents in each of the 12 ionization chambers characterize the proton Bragg curve when plotted as a function of preceding absorber material thickness. The thicknesses of the brass plates were carefully selected in order to obtain as many data points as possible in the Bragg peak region and less points in the entrance region where the dose gradient is small. It is possible to obtain the position of the distal 50 % dose point as a function of absorber thickness from these data points. This range value is then calibrated against range in water. A typical readout of the range monitor is also shown in figure 3.

For SOBP therapy the Bragg peak has to be spread out longitudinally. This is accomplished by rotating a propeller made up of different thicknesses of acrylic in the proton beam.<sup>6</sup> This device essentially superimposes a series of suitably weighted Bragg curves of reduced penetration on the full-range curve.

The photogrammetric patient positioning system (PPPS) used at the NAC makes use of real-time digital stereophotogrammetry techniques.<sup>7</sup> The PPPS is linked to the patient support system which is a computerized adjustable chair with five degrees of freedom. During the patient positioning stage, a set of three charge-coupled device (CCD) TV cameras captures video images, through a frame-grabber, of retroreflective markers on the patient's head. The positions of these markers are used to determine the patient's current position relative to the beam line and hence the translations and rotations required to move the patient into the final treatment position. Eight CCD video cameras are installed in the treatment room at suitable positions around the isocentre i.e. at different heights and angles to the beam line. During the initial stages of operation, it became apparent that these CCD cameras are quite susceptible to radiation damage. After careful investigations and some microdosimetric measurements<sup>8</sup> in and out the beam, it was concluded that the damage to the cameras was mainly due to protons scattered off the beam line and hitting the cameras directly. The occluding rings and second scatterer were the main source of scattered protons. Additional collimators as well as a 200 mm thick concrete brick wall were installed at the positions indicated in figure 1. Subsequent measurements showed that all the cameras are now being exposed to a similar dose rate during treatment which is approximately 8 times less than the highest dose rate, measured at a camera position before the shielding was installed.

### 3 Beam data

A series of depth dose curves for different diameter beams measured in water with a  $0.01 \text{ cm}^3$  air-filled tissue-equivalent thimble ionization chamber is shown in Figure 4. These curves were measured with all the modification devices, except the modulator propeller (see below) in the beam.

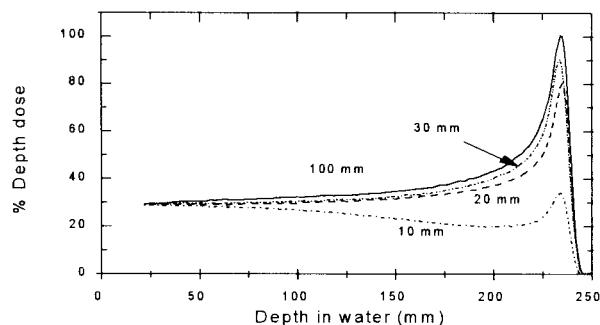


Figure 4: Depth dose curves for different field diameters.

A significant deterioration of the Bragg peak is evident as the diameter of the beam decreases below 20 mm. This effect is entirely due to scattering of the protons out of the

beam. The FWHM of the Bragg peak for the 10 cm diameter beam is 2.4 cm, while the 90% to 10% and 80% to 20% distal fall-offs are 0.60 and 0.40 cm respectively. The entrance to peak ratio is 0.28. Figure 5 shows the proton beam penumbrae at different depths as a function of field diameter for an unmodulated beam. It is clear that there is no significant field size effect on the penumbrae at shallow depths.

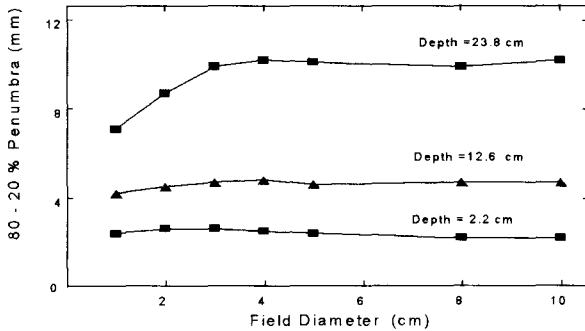


Figure 5: Proton beam penumbrae at different depths as a function of field diameter.

Figure 6 shows the penumbrae for a 50 mm diameter collimator as a function of depth for different degraded beams as well as those for an 8 MV x-ray beam. It is evident that the degraders have a significant effect on the proton beam penumbra which has to be taken into account in the treatment planning process. The change in penumbra will most probably be reduced if double or sandwich scatterers are used but it will adversely affect the penumbra at shallow depths for beams with longer ranges. It is interesting to note that the penumbra for the NAC proton therapy beam is always better than that for a 8 MV x-ray beam except for ranges greater than 200 mm which are never used for intracranial treatments.

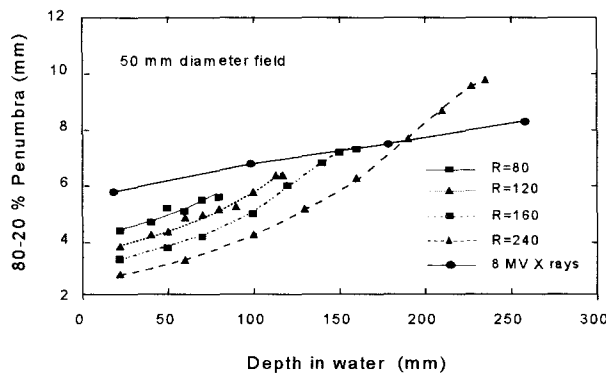


Figure 6: Proton beam penumbrae for a 50 mm diameter collimator as a function of depth for different degraded beams as well as those for an 8 MV x-ray beam.

Figure 7 shows a series of SOBPs measured for the 50 mm modulator propeller in a 50 mm diameter circular field for

different ranges. All the propellers for the NAC beam line were designed to give a dose uniformity of less than 1 % over the flat region of the SOBPs for a range of 120 mm in water. The changes in dose uniformity across the flat region of the SOBPs as a function of range is less than  $\pm 2.5\%$  for all the propellers used.

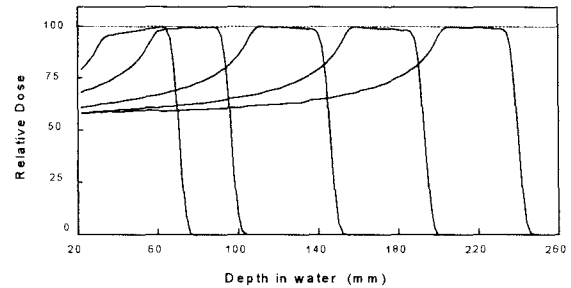


Figure 7: SOBPs for a 50 mm modulator propeller in a 50 mm diameter circular field for different ranges in water.

#### 4. Conclusions

Although the current beam delivery system of the NAC's proton therapy facility was designed for plateau irradiations, it was possible to adapt the same basic layout for SOBP treatments. The characteristics of the SOBP beams obtained are well within standard clinical specifications and compare favourably with those at other high energy proton treatment facilities. The double feedback system for controlling the clinical beam works very effectively. The additional collimators that were installed significantly decreased the radiation damage to the CCD cameras. The range monitor affords a real time check on the proton beam energy which is very important for SOBP treatments. Future investigations will include a proper assessment of the beam line layout for SOBP treatments using both theoretical calculations and experimental results. This might result in the use of double or sandwich degraders and propellers to minimize the changes in beam parameters as a function of beam degradation and modulation.

#### 5. References

1. D T L Jones, A N Schreuder, J E Symons and M Yudelev, *Hadrontherapy in Oncology*, 307 (1994)
2. A.M. Koehler, R.J. Schneider and J.M. Sisterson, *Med. Phys.* 4(4), 297 (1977)
3. B. Gottschalk, Personal Communication 1992.
4. S Vynckier, D.E. Bonnett and D.T.L. Jones, *Radioth. Oncol.* 20, 53 (1991).
5. S Vynckier, D.E. Bonnett and D.T.L. Jones, *Radioth. Oncol.* 32, 174 (1994).
6. A M Koehler, R J Schneider and J M Sisterson, *Nucl. Instr. and Meth.* 131, 437 (1975).
7. K.F. Bennett, H. Ruther, G. van der Vlugt and A.D.B. Yates, *S Afr J Sci*, 90,370 (1994).
8. P.J. Binns, Personal Communication 1994.